Supplemental Results

Overexpression of Gsk3 reverses inhibition by lithium

We tested whether raising the overall level of GSK-3 protein would increase substrate phosphorylation in the presence of lithium. A 50% increase in recombinant GSK-3 protein restores substrate phosphorylation in the presence of LiCl (1 mM) to control levels in vitro (Supplemental figure 1A). We then examined the endogenous GSK-3 substrates glycogen synthase (GS) and ß-catenin. GS is constitutively phosphorylated by GSK-3 (1) and this can be detected under basal conditions in HEK293T cells (Supplemental figure 1B); lithium is predicted to inhibit phosphorylation at this site. ß-catenin, an integral component of the Wnt signaling pathway, is also constitutively phosphorylated by GSK-3, leading to rapid degradation of ß-catenin and constitutive suppression of Wnt signaling; thus lithium inhibition of GSK-3 stabilizes ß-catenin and robustly activates Wnt-dependent transcription (2-4).

As expected, lithium inhibited phosphorylation of GS in HEK293T cells, as demonstrated by western blot with a phospho-specific antibody (Supplemental figure 1B, upper panel) without altering the abundance of GS protein (Supplemental figure 1B, middle panel). Lithium also activated the Wnt reporter OT-luciferase >700-fold (Supplemental figure 1C). Increasing *Gsk3b* expression restored phosphorylation of GS in the presence of lithium to control levels (Supplemental figure 1B) and reversed the activation of Wnt/ß-catenin-dependent transcription by lithium by more than 3-fold (Supplemental figure 1C). Overexpression of *Gsk3b* also restores phosphorylation of tau protein in 293T cells in the presence of lithium (data not shown). These data confirm that overexpression of *Gsk3b* can reverse the biochemical and molecular effects of lithium.

We suggest that elevating GSK-3 concentration overcomes the effects of lithium for two reasons. First, raising total enzyme concentration ($[E_T]$) is expected to increase both initial velocity (v_o) and Vmax at a given concentration of inhibitor. Second, as discussed in the text, GSK-3 positively regulates its own activity by antagonizing its N-terminal phosphorylation, and this positive feedback allows small increases in cellular GSK-3 activity to be amplified and thus attenuate sensitivity to lithium (4, 5).

Elevated GSK-3 activity in the cortex and striatum of Gsk3b transgenic mice

To assess GSK-3 activity in the brain of *wild-type* and *Gsk3b* transgenic mice, we adapted a previously described assay for GSK-3 activity in whole cell lysates (6). Brains were dissected from wild-type, *PrpGsk3b*^{L56} and *PrpGsk3b*^{L64} mice (five mice per genotype) and cytosolic extracts were prepared from cortex and striatum as described in Supplemental Methods. Phosphorylation of a GSK-3 specific substrate (GS-2, a primed glycogen synthase peptide) was measured in the absence or presence of LiCl, and GSK-3 activity (as [total phosphorylation of GS2 – phosphorylation in the presence of LiCl] (6)) was plotted in Supplemental Figure 2. The data show the mean activity from 5 mice per group. GSK-3 activity in the striatum of both *Gsk3b* transgenic mice increased by ~20%. Similarly, activity was increased in the cortex of *prpGsk3b*^{L56} and *prpGsk3b*^{L64} mice. We note, however, that while we detect higher GSK-3ß-his expression in all brain regions tested from *prpGsk3b*^{L56} vs. *prpGsk3b*^{L64} mice (Figure 1B), we are unable to establish a difference in overall enzyme activity when comparing these two transgenic lines, perhaps because of individual variation in the samples and/or because the activity assay measures the total activity contributed by both GSK-3 isoforms from all cell types (as opposed to Prp-dependent expression of the transgene) within the examined tissue.

Overexpression of Gsk3 does not alter inositol levels in vivo

In *Saccharomyces cerevisiae*, GSK-3 also regulates inositol synthesis (7). As an alternative hypothesis for lithium action is that lithium inhibits inositol recycling through inhibition of inositol monophosphatase (8), a plausible mechanism for the attenuation of lithium-sensitive behaviors in Gsk3b transgenic mice is that overexpression of Gsk3 increases inositol synthesis, restoring inositol levels and inositol-dependent signaling in lithium treated animals. Consistent with this hypothesis, we have shown previously that the developmental effects of expression of a dominant negative form of Gsk3 in Xenopus laevis can be reversed by coinjection of exogenous inositol (2). We therefore tested whether overexpression of *Gsk3b* alters inositol levels in mouse brain. Cortex, striatum, and hippocampus were dissected from wild-type, *PrpGsk3b*^{L56} and *PrpGsk3b*^{L64} mice and inositol levels were measured by GC-MS as described previously (9). As shown in Supplemental Figure 3, there was no difference in inositol levels in *wild-type* or transgenic mice. While variation in inositol within more restricted cell populations or subcellular domains remains possible, taken together with our previous findings that reduction of inositol in the brain does not reproduce lithium-like behaviors, we conclude that the behavioral effects of lithium and Gsk3b overexpression are not caused by global changes in inositol abundance.

Rescue of behavioral phenotypes in Gsk3b$^{+/-}$ mice

Loss of one copy of *Gsk3b* is phenocopied by lithium in multiple behavioral tests (10-12), and similar effects on behavior are also observed with homozygous loss of *Gsk3a* (13). However, while these behavioral phenotypes provide a strong correlation between behavioral effects of lithium and inhibition of GSK-3, the possibility remains that the behaviors arise from off-target effects, such as a cryptic mutation introduced by targeting *Gsk3b* or closely linked polymorphisms that are not related to *Gsk3b*. For these reasons,

it is essential to validate these findings by replacing *Gsk3b* in the context of the *Gsk3b*$^{+/-}$ mouse and test whether this restores normal behaviors. Thus, *PrpGsk3b* mice were crossed to *Gsk3b*$^{+/-}$ mice and progeny (wild-type, *PrpGsk3b*, *Gsk3b*$^{+/-}$ heterozygotes, and the bigenic rescue line (*PrpGsk3b;Gsk3b*$^{+/-}$)) were tested in the FST, EXPL, and open field behaviors.

Gsk3b$^{+/-}$ mice showed reduced time immobile in the FST compared to wt mice (Supplemental figure 4A), consistent with previous results and similar to treatment with lithium (10, 14) and other small molecule GSK-3 inhibitors (15, 16). Restoring *Gsk3b* expression to *Gsk3b*$^{+/-}$ heterozygotes (*PrpGsk3b;Gsk3b*$^{+/-}$) corrected the behavioral phenotype in the FST, strongly suggesting that this behavior arises specifically through reduced *Gsk3b* expression, rather than an off-target genetic defect. Importantly, *PrpGsk3b* transgenic mice were unaffected in the FST, indicating that this level of overexpression does not by itself perturb behavior in the FST.

Furthermore, exploratory behavior is reduced in *Gsk3b*$^{+/-}$ mice, as reported previously, but is restored to wild type levels in bigenic *PrpGsk3b;Gsk3b*$^{+/-}$ mice (Supplemental figure 4B), again indicating rescue of the behavioral phenotype in *Gsk3b*$^{+/-}$ mice. *PrpGsk3b* mice also demonstrated increased hole pokes at baseline (Supplemental figure 4B; see also figure 2C), suggesting that this behavior is sensitive to both increased and decreased GSK-3ß activity. Importantly, no changes in total activity were observed during the exploratory behavior for any of the above genotypes (WT, *PrpGsk3b*, *Gsk3b*$^{+/-}$, and *PrpGsk3b;Gsk3b*$^{+/-}$), arguing against changes in overall activity that could confound analysis of these and other behaviors (Supplemental figure 4C; see also Supplemental figure 5).

Baseline behavior in Gsk3b transgenic mice

Locomotor activity in the open field, time spent in the center versus periphery of the open field (Supplemental Figure 5), latency to drop from an accelerating rotorod, home cage behavior, and general state of *Gsk3b* transgenic mice were indistinguishable from their wild-type littermates, indicating no overt physiological or behavioral state changes in *Gsk3b* overexpressing mice.

Supplemental Methods

GSK-3 assays

In vitro GSK-3 assays were performed as described (17) except kinase buffer was 150mM Tris pH7.5, 5 mM DTT, 0.5 mM $MgCl_2$, 100 µM ATP and reactions were run for 10 minutes at 30ºC. LiCl was added to a final concentration of 1mM. GSK-3ß enzyme was purchased from New England Biolabs. For cell-based GSK-3 assays, 293T cells with a stably incorporated ß-catenin/Tcf-dependent transcription reporter (293OT cells) were used (4, 18). Cells were maintained in 10% FBS in DMEM plus 1% Penicillin and Streptomycin, plated in 6-well dishes at a density of 7.5 x 10^5 cells/well, allowed to adhere, and then transfected (Fugene) with pEGFP and pCS2 (vector control) or pCS2:XGSK3β (0.50 ug) overnight. The transfection efficiency was estimated to be >90% by GFP fluorescence. Twenty-four hours after transfection the medium was replaced with fresh medium containing 10mM LiCl or control medium. Cells were cultured overnight, lysed in Promega passive lysis buffer with protease and phosphatase inhibitors added, and subjected to immunoblot for detection of phospho-epitopes. Wnt reporter activation was determined by analysis of luciferase activity as described (4). Results are reported as relative light units (RLU) normalized to protein in each sample.

GSK-3 activity in striatal and cortical lysates was measured according to a previously described method (6) in which phosphorylation of a primed glycogen synthase peptide was measured with or without LiCl. Brains were dissected from five mice per genotype, homogenized in 20 mM HEPES pH 7.4, 1% Triton X-100, 100mM NaCl, 20mM NaF, 5mM EDTA, Sigma protease inhibitor cocktail (1:100), Sigma phosphatase inhibitor cocktails 2 and 3 (1:100), 2mM PMSF, 2uM Okadaic acid, 0.5uM microcystin, and adjusted to 0.8 mg/ml. Lysate (10µl) was added to an equal volume of 2X reaction mix for a final composition of 150mM Tris pH 7.5, 5mM DTT, 10mM $MgCl_2$, 0.1mM ATP (with 0.06 µCi/µl [^{32}P]-γ-ATP) with or without 200mM LiCl, as described previously (6), incubated at 30ºC for 10 minutes, and then reactions were stopped by spotting onto P-81 paper and immersing in cold 10mM H_3PO_4, washed in H_3PO_4, dried, and counted in a scintillation counter.

Inositol analyses in brain

Inositol concentration in cortex, striatum, and hippocampus was measured using GC-MS and an isotope dilution method, as described previously (9, 19). Brain samples were weighed and homogenized in 500µl CH_3OH:$CHCl_3$ (50:50) after addition of 2µl of 10mM [$^2H_6$]myo-inositol. The aqueous phase was extracted twice with $CHCl_3$ and 50µl of the aqueous phase was dired under N2 and derivatized overnight with N,O-bis(trimethylsilyl) trifluoroacetamide/ trimethylchlorosilane (BSTFA-1% TMCS, Sigma Aldrich, St. Louis, MO) to convert endogenous myo-inositol and the internal standard to trimethylsilyl derivatives to be analyzed by GC-MS using an Agilent 7890A/5975 system. GC separation was performed using a 30m x 250 µm (i.d.) x 0.25 µm film HP-5MS column (J&W Scientific). Derivatized extract (1 µl) was injected into the GC-MS using splitless mode. The column was kept at an initial temperature of 125ºC for 1 minute and increase to 150ºC at a rate of 20º/min, then ramped to 215ºC at a rate of 4º/min, reaching final

temperature of 300ºC by 30ºC/min, and kept at this final temperature for 5 min. Prominent ion fragments at m/z 318 and m/z 321 observed for both compounds were monitored, and the integrated ion ratios m/z 318 to m/z 321 (myo-inositol/[$^2H_6$]myo-inositol) were used for quantification of myo-inositol in the samples.

Open field activity and Accelerating Rotorod

To assess the general state of the mice and verify that the transgene did not alter neuromuscular function required to perform behaviors, we measured open field activity and accelerating rotorod. Open field activity was assessed in a 14 x 14 inch arena (San Diego Instruments, San Diego, CA) fitted with photocells to count rearing, center activity, peripheral activity, and total activity in a 10 min trial. As a measure of strength and neuromuscular coordination, mice were placed on a rotorod (Ugo Basile) that accelerated at a constant rate from 4-40 rpm in 5 minutes. The latency to fall was recorded. No differences in performance in the rotorod or open field were observed among the genotypes tested.

Supplemental References

1. Doble, B.W., and Woodgett, J.R. 2003. GSK-3: tricks of the trade for a multi-tasking kinase. *Journal of Cell Science* 116:1175-1186.
2. Hedgepeth, C., Conrad, L., Zhang, Z., Huang, H., Lee, V., and Klein, P. 1997. Activation of the Wnt Signaling Pathway: A Molecular Mechanism for Lithium Action. *Devel. Biol.* 185:82-91.
3. Stambolic, V., Ruel, L., and Woodgett, J. 1996. Lithium inhibits glycogen synthase kinase-3 activity and mimics wingless signalling in intact cells. *Curr. Biol.* 6:1664-1668.
4. Zhang, F., Phiel, C.J., Spece, L., Gurvich, N., and Klein, P.S. 2003. Inhibitory phosphorylation of glycogen synthase kinase-3 (GSK-3) in response to lithium. Evidence for autoregulation of GSK-3. *J Biol Chem* 278:33067-33077.
5. De Sarno, P., Li, X., and Jope, R.S. 2002. Regulation of Akt and glycogen synthase kinase-3beta phosphorylation by sodium valproate and lithium. *Neuropharmacology* 43:1158-1164.
6. Ryves, W.J., Fryer, L., Dale, T., Harwood, A.J. 1998. An assay for glycogen synthase 3 (GSK-3) for use in crude cell extracts. *Anal. Biochem.* 264:124-127.
7. Azab, A.N., He, Q., Ju, S., Li, G., and Greenberg, M.L. 2007. Glycogen synthase kinase-3 is required for optimal de novo synthesis of inositol. *Mol Microbiol* 63:1248-1258.
8. Berridge, M.J., Downes, C.P., and Hanley, M.R. 1989. Neural and developmental actions of lithium: a unifying hypothesis. *Cell* 59:411-419.
9. Shaldubina, A., Johanson, R.A., O'Brien, W.T., Buccafusca, R., Agam, G., Belmaker, R.H., Klein, P.S., Bersudsky, Y., and Berry, G.T. 2006. SMIT1 haploinsufficiency causes brain inositol deficiency without affecting lithium-sensitive behavior. *Molecular Genetics & Metabolism* 88:384-388.
10. O'Brien, W.T., Harper, A.D., Jove, F., Woodgett, J.R., Maretto, S., Piccolo, S., and Klein, P.S. 2004. Glycogen synthase kinase-3beta haploinsufficiency mimics the behavioral and molecular effects of lithium. *Journal of Neuroscience* 24:6791-6798.
11. Beaulieu, J.M., Sotnikova, T.D., Yao, W.D., Kockeritz, L., Woodgett, J.R., Gainetdinov, R.R., and Caron, M.G. 2004. Lithium antagonizes dopamine-dependent behaviors mediated by an AKT/glycogen synthase kinase 3 signaling cascade. *Proceedings of the National Academy of Sciences of the United States of America* 101:5099-5104.
12. Beaulieu, J.M., Marion, S., Rodriguiz, R.M., Medvedev, I.O., Sotnikova, T.D., Ghisi, V., Wetsel, W.C., Lefkowitz, R.J., Gainetdinov, R.R., and Caron, M.G. 2008. A beta-arrestin 2 signaling complex mediates lithium action on behavior. *Cell* 132:125-136.
13. Kaidanovich-Beilin, O., Lipina, T.V., Takao, K., van Eede, M., Hattori, S., Laliberté, C., Khan, M., Okamoto, K., Chambers, J.W., Fletcher, P.J., et al. 2009. Abnormalities in brain structure and behavior in GSK-3alpha mutant mice. *Mol Brain* 2:35.
14. Beaulieu, J.M., Zhang, X., Rodriguiz, R.M., Sotnikova, T.D., Wetsel, W.C., Gainetdinov, R.R., and Caron, M.G. 2008. Reply to Belmaker et al.: GSK3 haploinsufficiency results in lithium-like effects in the forced-swim test. *Proc Natl Acad Sci U S A* 105:E24.
15. Gould, T.D., Einat, H., Bhat, R., and Manji, H.K. 2004. AR-A014418, a selective GSK-3 inhibitor, produces antidepressant-like effects in the forced swim test. *International Journal of Neuropsychopharmacology* 7:387-390.

16. Kaidanovich-Beilin, O., Milman, A., Weizman, A., Pick, C.G., and Eldar-Finkelman, H. 2004. Rapid antidepressive-like activity of specific glycogen synthase kinase-3 inhibitor and its effect on beta-catenin in mouse hippocampus. *Biological Psychiatry* 55:781-784.
17. Klein, P.S., and Melton, D.A. 1996. A molecular mechanism for the effect of lithium on development. *Proc. Nat'l. Acad. Sci. U.S.A.* 93:8455-8459.
18. Korinek, V., Barker, N., Morin, P.J., van Wichen, D., de Weger, R., Kinzler, K.W., Vogelstein, B., and Clevers, H. 1997. Constitutive transcriptional activation by a beta-catenin-Tcf complex in APC-/- colon carcinoma. *Science* 275:1784-1787.
19. Berry, G.T., Wu, S., Buccafusca, R., Ren, J., Gonzales, L.W., Ballard, P.L., Golden, J.A., Stevens, M.J., and Greer, J.J. 2003. Loss of murine Na+/myo-inositol cotransporter leads to brain myo-inositol depletion and central apnea. *Journal of Biological Chemistry* 278:18297-18302.

Supplemental Figure Legends

Supplemental Figure 1. Overexpression of GSK-3 overcomes inhibition by LiCl. (A) In vitro GSK-3 assay showing phosphorylation of glycogen synthase peptide GS-2 in the absence (light gray bar) or in the presence (dark gray bars) of LiCl (1 mM). The amount of recombinant GSK-3 added per reaction was increased by 1.5- and 2-fold, as indicated. Initial velocity as moles of phosphate incorporated per mole of substrate per minute is shown. (B) 293T-OT cells were transfected with control vector or plasmid encoding GSK-3ß, incubated for 24 hours, treated with LiCl (0, 5, or 10 mM) overnight, and harvested for immunoblot to detect phosphorylated GS (phospho-GS, upper panel), total GS (middle panel), or GSK-3α and ß (lower panel). (C) 293T-OT cells were treated with LiCl (10 mM) overnight and then assayed for luciferase activity, shown as relative light units (RLU)/ug of total protein. The mean from three independent experiments is shown.

Supplemental Figure 2. GSK-3 activity in striatum and cortex of *Wt* and *PrpGsk3b* mice. Striatum and cortex were dissected from *Wt, PrpGsk3b*^{L56}, and *PrpGsk3b*^{L64} mice and cytosolic extracts were assayed for lithium-sensitive protein kinase activity toward a pre-phosphorylated GS-2 peptide, as described (6). The histograms represent mean activity ± SEM for each genotype (n = 5 mice per group). Lithium-insensitive protein kinase activity (background) in the samples was similar in wild-type vs. transgenic samples (not shown).

Supplemental Figure 3. Myo-inositol level is not altered in *PrpGsk3b* mice. Cortex, striatum, and hippocampus were dissected from *Wt, PrpGsk3b*^{L56}, and *PrpGsk3b*^{L64} mice and myo-inositol (Ins) was measured by GC-MS, as described (9). The histograms

represent mean Ins ± SEM for each genotype (n = 5 mice per group). There were no significant differences in mean inositol among the groups.

Supplemental Figure 4. Transgenic expression of *Gsk3b* rescues the behavioral phenotypes of *Gsk3b*$^{+/-}$ mice. *Wt*, *PrpGsk3b*, *Gsk3b*$^{+/-}$, and the bigenic *PrpGsk3b;Gsk3b*$^{+/-}$ mice were tested in (A) the FST (n= 30, 34, 9, and 8 respectively), (B) EXPL (n= 35, 29, 10, and 9 respectively), and (C) total activity (n= 14, 8, and 8, respectively). *p < 0.05 compared to wild type, #p < 0.05 compared to *Wt* + LiCl.

Supplemental Figure 5. Open field activity is not affected in *PrpGsk3b* mice. *Wt*, *PrpGsk3b*^{L56}, and *PrpGsk3b*^{L64} mice were tested for total activity in the open field. Transgenic mice were not different from control.

Supplemental Figure 6 The GSK-3 inhibitor AR-AO14418 disrupts the AKT/PP2A/ß-arrestin-2 complex, similar to LiCl and 6BIO. Striatal homogenates from *Wt* mice were exposed to the GSK-3 inhibitors LiCl, 6-BIO, and AR-AO14418 (or DMSO as a control) and then subjected to immunoprecipitation (IP) with anti-Akt antibody followed by immunoblotting (IB) for PP2A (upper panel) or Akt (lower panel). See Figure 3A and Figure 3B.

Supplemental Figure 1

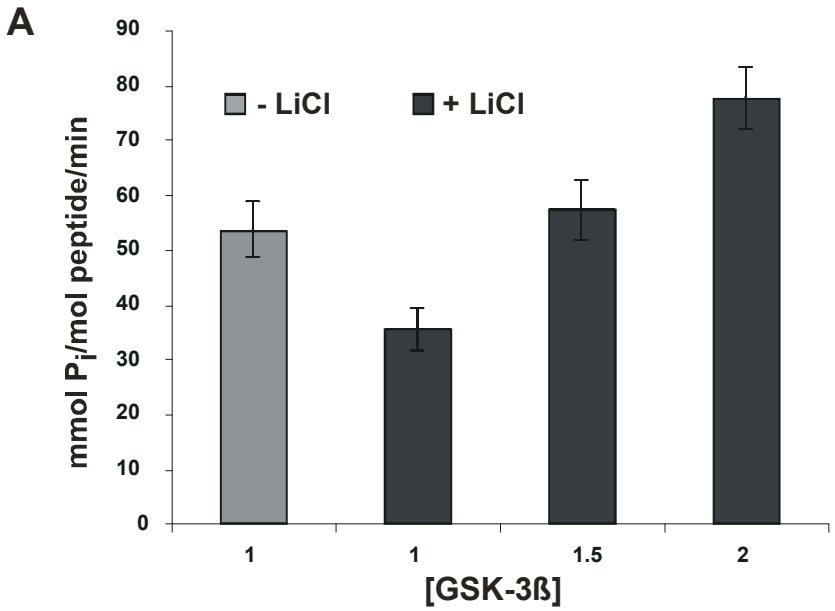

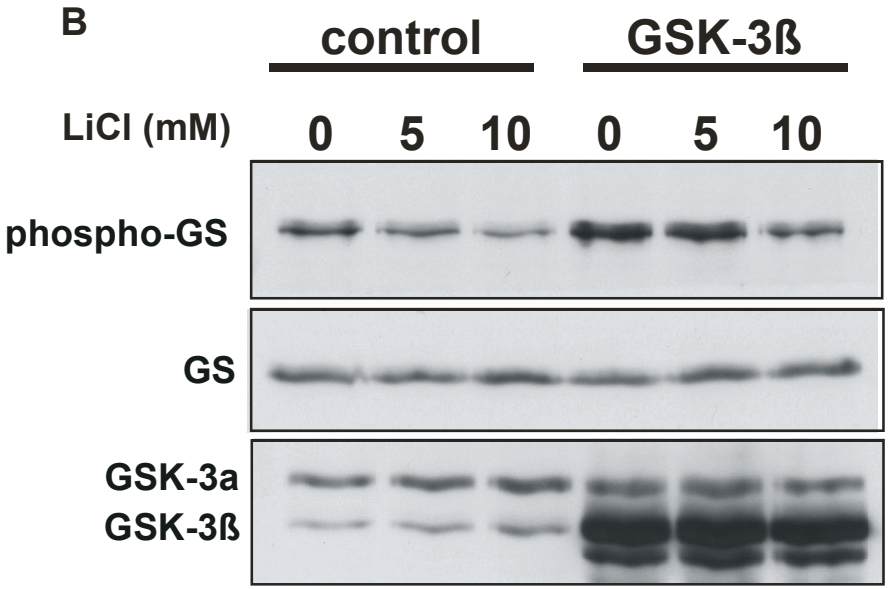

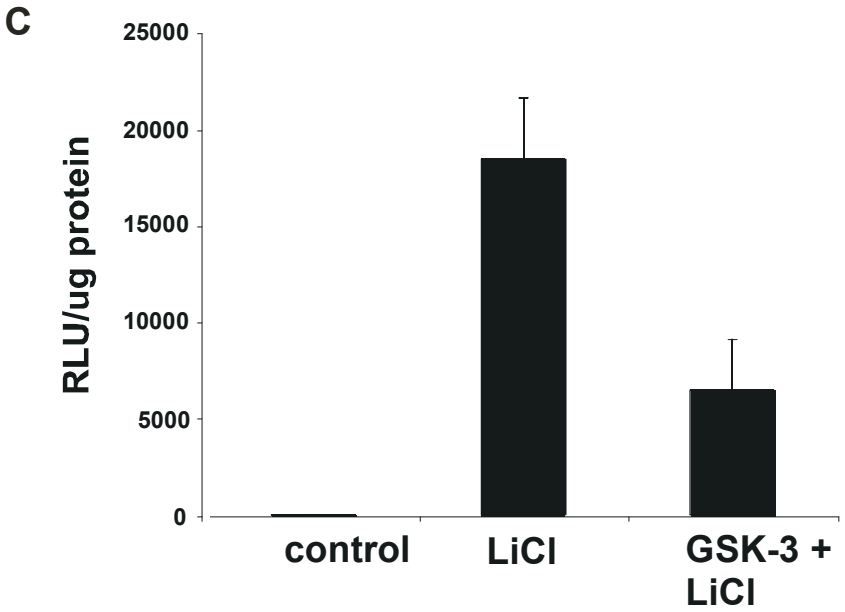

Supplemental Figure 1.
Overexpression of GSK-3 overcomes inhibition by LiCl.

(A) In vitro GSK-3 assay showing phosphorylation of glycogen synthase peptide GS-2 in the absence (light gray bar) or in the presence (dark gray bars) of LiCl (1 mM). The amount of recombinant GSK-3 added per reaction was increased by 1.5- and 2-fold, as indicated. Initial velocity as mmoles of phosphate incorporated per mole of substrate per minute is shown. (B) 293T-OT cells were transfected with control vector or plasmid encoding GSK-3ß, incubated for 24 hours, treated with LiCl (0, 5, or 10 mM) overnight, and harvested for immunoblot to detect phosphorylated GS (phospho-GS, upper panel), total GS (middle panel),or GSK-3α and ß (lower panel). (C) 293T-OT cells were treated with LiCl (10 mM) overnight and then assayed for luciferase activity, shown as relative light units (RLU)/ug of total protein. The mean from three independent experiments is shown.

Supplemental Figure 2

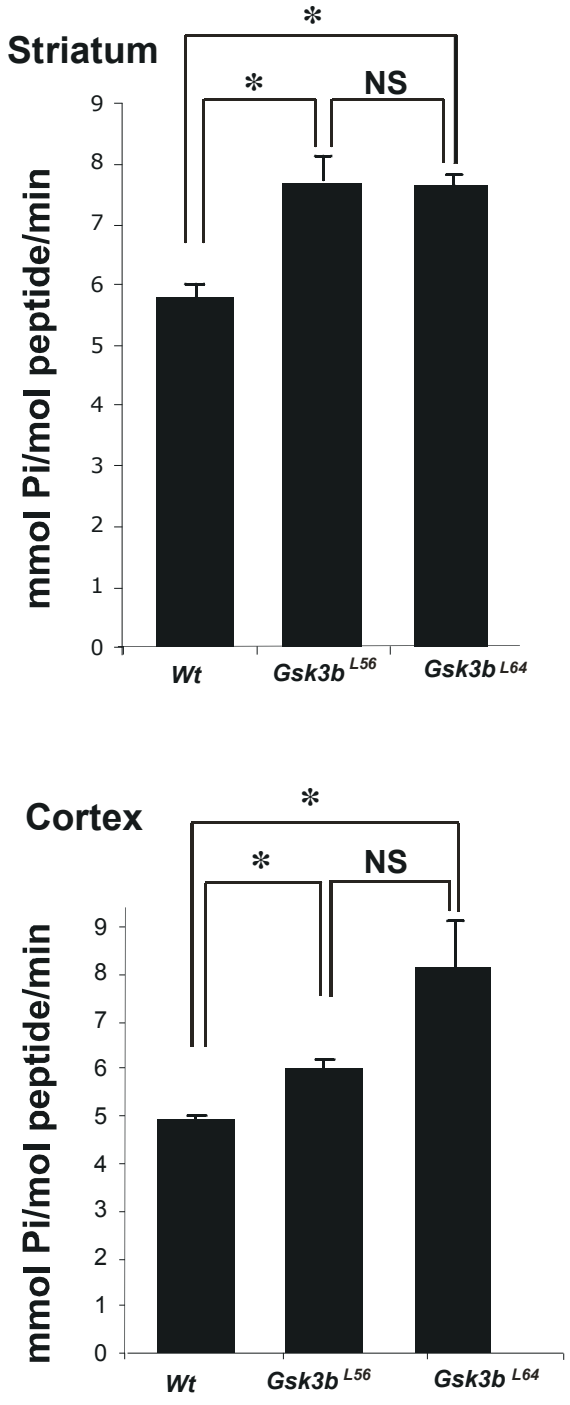

Supplemental Figure 2. GSK-3 activity in striatum and cortex of *Wt* and *PrpGsk3b* mice. Striatum and cortex were dissected from *Wt, PrpGsk3bL56*, and *PrpGsk3bL64* mice and cytosolic extracts were assayed for lithium-sensitive protein kinase activity toward a pre-phosphorylated GS-2 peptide, as described (6). The histograms represent mean activity ± SEM for each genotype (n = 5 mice per group). Lithium-insensitive protein kinase activity (background) in the samples was similar in wild-type vs. transgenic samples (not shown).

Supplemental Figure 3

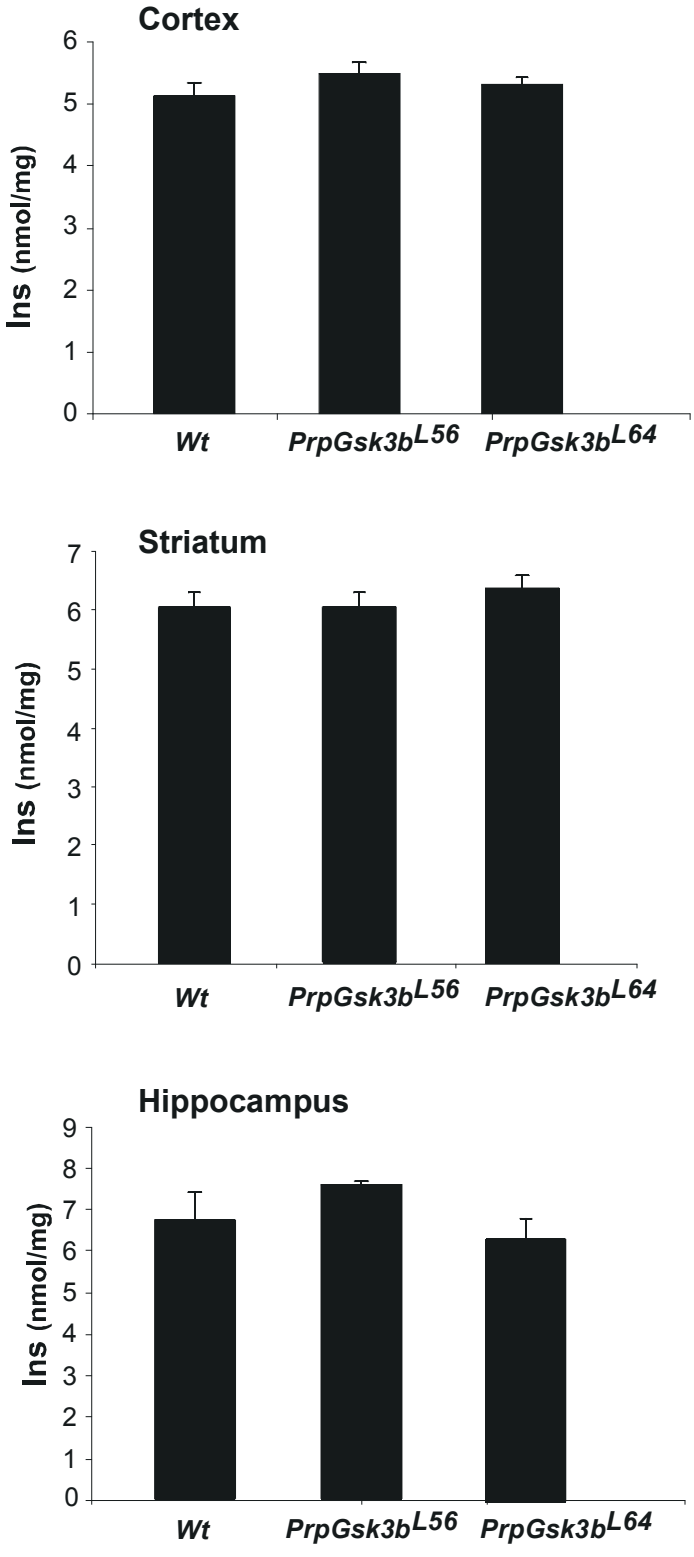

Supplemental Figure 3. Myo-inositol levels in cortex, striatum, and hippocampus are not altered in *Gsk3b* overexpressing mice. Cortex, striatum, and hippocampus were dissected from *Wt, PrpGsk3b^{L56}*, and *PrpGsk3b^{L64}* mice and myo-inositol (Ins) was measured by GC-MS, as described (9). The histograms represent mean Ins ± SEM for each genotype (n = 5 mice per group). There were no significant differences in mean Ins among the groups.

Supplemental Figure 4

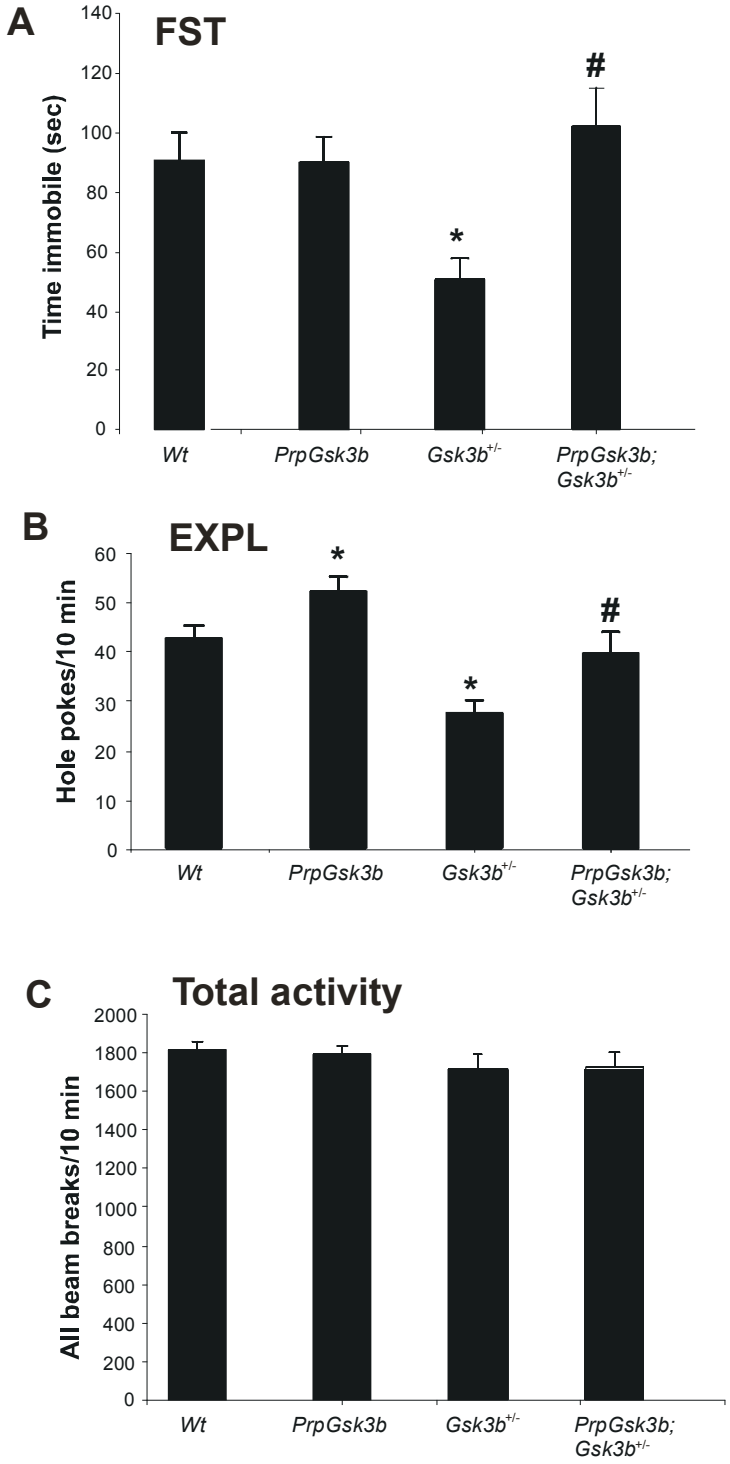

Supplemental Figure 4. The *Gsk3b* transgene rescues behavioral phenotypes in *Gsk3b*$^{+/-}$ mice. *Wt*, *PrpGsk3b*^{L56}, *Gsk3b+/-*, and the bigenic *PrpGsk3b*^{L56}*;Gsk3b+/-* mice were tested in (A) the FST (n= 30, 34, 9, and 8 respectively), (B) EXPL (n= 35, 29, 10, and 9 respectively), and (C) total activity (n= 14, 8, and 8, respectively). *p < 0.05 compared to wild type, #p < 0.05 compared to *Wt* + LiCl.

Supplemental Figure 5

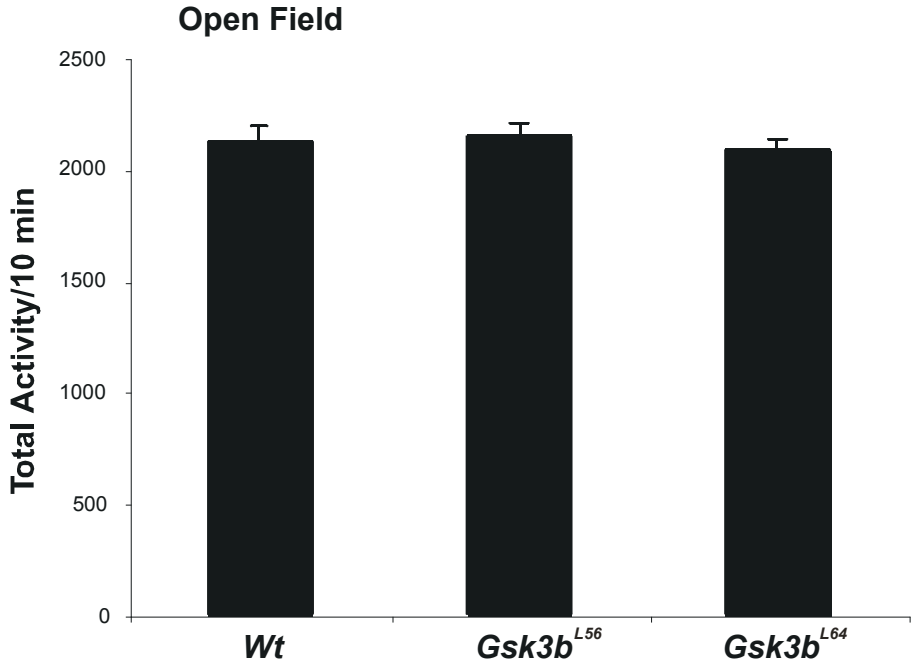

Supplemental Figure 5. *Gsk3b* transgenic mice behave normally in the open field. *Wt*, *PrpGsk3b*^{L56}, and *PrpGsk3b*^{L64} mice were tested for total activity in the open field. Transgenic mice were not different from control.

Supplemental Figure 6

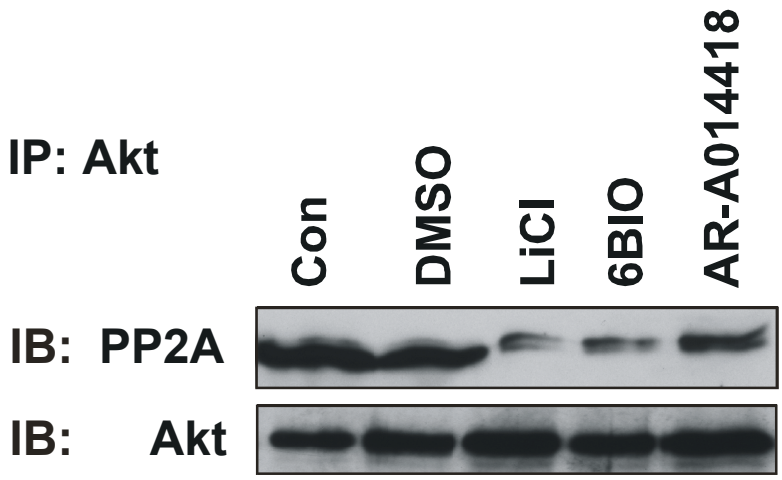

Supplemental Figure 6 The GSK-3 inhibitor AR-AO14418 disrupts the AKT/PP2A/ß-arrestin-2 complex, similar to LiCL and 6BIO. Striatal homogenates from *Wt* mice were exposed to the GSK-3 inhibitors LiCl, 6-BIO, and AR-AO14418 (or DMSO as a control) and then subjected to immunoprecipitation (IP) with anti-Akt antibody followed by immunoblotting (IB) for PP2A (upper panel) or Akt (lower panel). See Figure 3A and Figure 3B